

ADHESION OF THERMALLY SPRAYED COATINGS – AWRA CONTRACT 81

By C.C. Berndt* and R. McPherson*

ABSTRACT

A fracture mechanics approach to the adhesion of plasma sprayed coatings provides insights into the mechanism of adhesion. Thus the strain energy release rate for adhesive or cohesive failure may be related to microstructural features of coatings. Plastic deformation of coating lamellae and the effectiveness of contact between impinging droplets and the substrate or previously solidified material are important factors in determining coating properties.

1 INTRODUCTION

A primary requirement for any protective coating is good adherence to the substrate and the adhesion of plasma sprayed coatings has been a topic of considerable interest for some time. There has been little agreement however between the proponents of various theories for the mechanism of adhesion and the subject remains controversial. The bonding mechanisms at the coating substrate interface have been classified [1] as mechanical (associated with mechanical interlocking of particles to the roughened substrate), physical (Van der Waal's forces) or chemical (interdiffusion between coating and substrate). These theories have been largely conjectural with limited experimental evidence and they have not been successful in explaining many features of the behaviour of plasma sprayed coatings, for example the reason why metallic subcoats improve the adhesion of ceramic coatings.

A new approach to the problem has recently been developed which shows promise of a better understanding of the adhesion of plasma sprayed coatings [2-4]. This places emphasis on the difficulty of removal of the coating and is based on measurements of the energy associated with the propagation of cracks along the coating substrate interface (separation at the interface) and also at the coating-subcoat interface or within the coating itself. The experimental techniques used are based on those of classical fracture mechanics and the parameters determined are then related to microstructural factors controlling mechanical behaviour.

The fracture mechanics approach is based on an energy balance criterion for crack growth in a solid body [5]. As a crack grows the mechanical energy decreases and the surface energy increases; the equilibrium condition is given by $dU/d\ell = 0$ where U is total energy and ℓ is the crack length. The elastic strain energy (U_E) can be calculated if it is assumed that Hooke's law is obeyed and is given by $U_E = \frac{1}{2}F^2C$ where F is the tensile force and C is the elastic compliance. The strain energy release rate per unit width of crack front can be defined as $G = -dU_E/d\ell$, so that $G = WF^2 dC/d\ell$ for constant force. There is a critical value of strain energy release rate (G_c) for a cracked body at which the crack extends and this can be regarded as the fracture toughness of the material. For a completely brittle material the area of crack surface produced during advancement of the unit width crack is associated with a surface energy of 2γ so that $G_c = 2\gamma$. In most material however there are other contributions to G_c (plastic deformation, microcracking) so that it is usually much greater than 2γ .

There are a number of experimental techniques available which allow the fracture toughness parameter, G , to be determined. The work described in the present paper makes use of the double cantilever beam method to determine values of G for crack propagation within plasma sprayed composite specimens.

2 EXPERIMENTAL PROCEDURE

Mild steel substrates 150 x 20 x 6 mm were grit blasted with alumina along the narrow edge and plasma sprayed with $Al_2O_3-2.5\% TiO_2$ (Metco 101), Ni-4.5% Al (Metco 450) and mild steel (Metco 91) using a Plasmadyne SG-1B (SI) gun with the conditions shown in Table 1.

Composite coatings of Al_2O_3 on a Ni-Al subcoat were also prepared.

A support bar with the same dimensions as the specimen, and grit blasted along one edge, was attached to the coating using an epoxy adhesive layer (Araldite D with hardener 951) 1-2 mm thick as shown in Figure 1. Care was taken to produce a sound, defect free bond. A groove was machined in the vicinity of the coating substrate interface to control the crack path (along the interface or within the coating) and a saw cut, 0.2 mm wide, was introduced, as shown in Figure 1 to start the crack. The specimen was loaded in tension, through holes in the cantilever arms, at a cross head speed of 0.1 mm min^{-1} and the displacement of the arms measured using an extensometer positioned across the initial saw cut. The specimen was strained

TABLE 1 PLASMA SPRAYING CONDITIONS

Coating Material	Deposit Thickness (mm)	Gas Flow Rate $\ell \text{ min}^{-1}$		Power Input kW
		Ar	He	
Ni-4.5% Al (Metco 450)	0.5 – 2.0	28	–	18
$Al_2O_3-2.5\% TiO$ (Metco 101)	0.5	28	7	31
Mild Steel (Metco 91)	1.0	28	–	17

TABLE 2 STRAIN ENERGY RELEASE RATE (G) FOR VARIOUS COATINGS AND FRACTURE TYPES

Coating	Failure Type	$G \text{ (Jm}^{-2}\text{)}$		Standard Deviation
		Range	Mean	
Mild Steel	Adhesive	78-143	116	21
	Cohesive	155-375	261	71
Ni-Al	Adhesive	(> 1000)	–	–
	Cohesive	109-472	319	95
$Al_2O_3-TiO_2$	Adhesive	10-15	12	2
	Adhesive to Ni-Al subcoat	35-95	58	16
	Cohesive	16-25	21	5

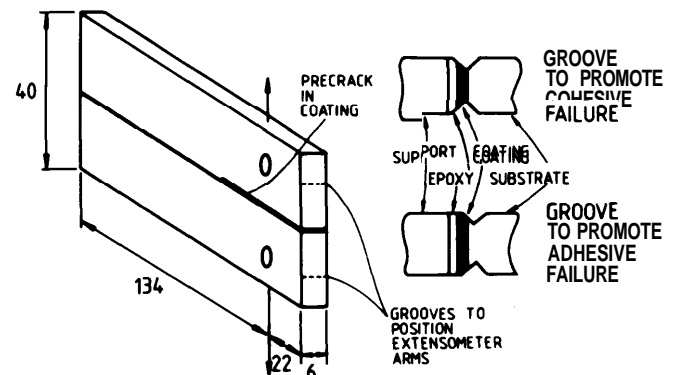


FIG 1 CONFIGURATION OF DOUBLE CANTILEVER BEAM COMPOSITE SPECIMEN

* Monash University.

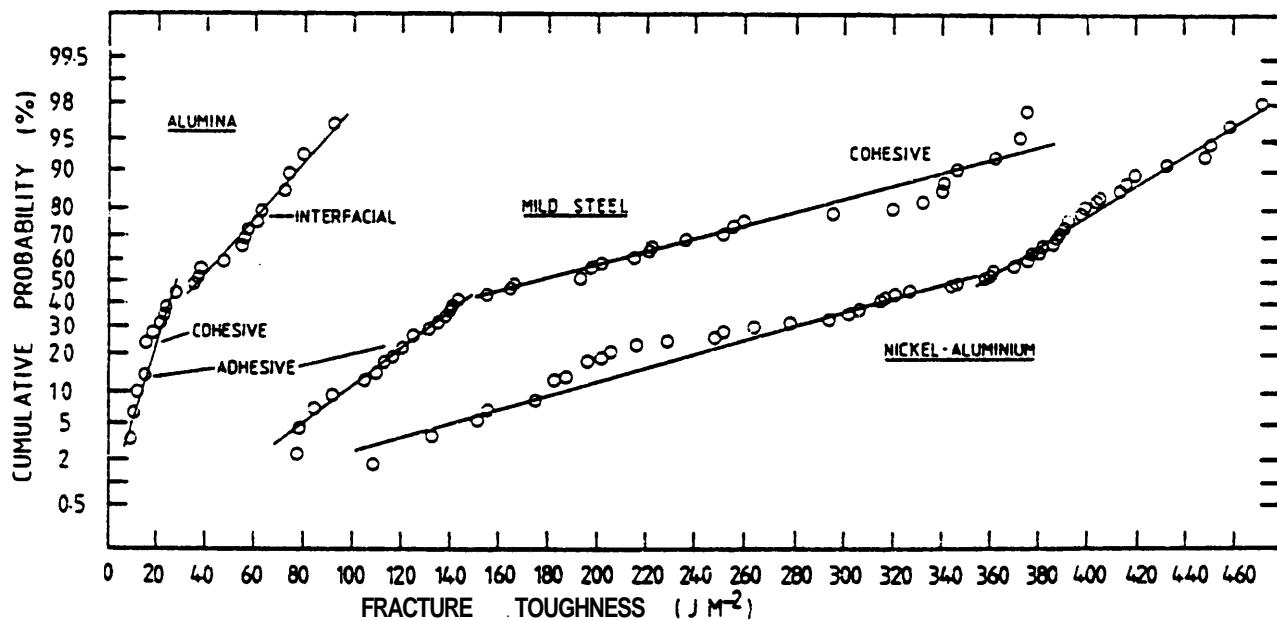


FIG 2 PROBABILITY PLOT OF FRACTURE TOUGHNESS DATA (G)

until a constant load was achieved, representing crack propagation, and then unloaded. This procedure was repeated several times for each specimen. The critical strain energy release rate, G_c , is given by

$$G = \frac{F_c^2}{2W} \frac{dc}{d\ell}$$

where F_c = critical force (N)
 W = crack width (M)
 c = specimen compliance (mN^{-1})
 ℓ = crack length (m)

To determine G the change of specimen compliance with crack length must be known. A calibration curve of specimen compliance versus crack length was constructed using specimens with artificial cracks of known length. For the configuration used this gave

$$G = 4.193 \times 10^{-2} F_c^2 \ell^{0.989}$$

A series of G values was found for each specimen from the peak force values and the compliance determined from unloading lines.

The fracture surfaces were examined by scanning electron microscopy to determine the nature of the failure and to distinguish between cohesive fracture (within the coating) and adhesive fracture (in the vicinity of the substrate coating interface).

3 RESULTS

A wide range of values of G was obtained for each mode of failure and material as shown in Table II. Adhesive failure of Ni-Al was difficult to obtain and only one extremely high value ($>1000 Jm^{-2}$) was observed. Cumulative probability plots of the data showed bimodal distributions for $Al_2O_3-TiO_2$ and steel coatings with the two branches of the plot corresponding to adhesive or cohesive failure respectively, as shown in Figure 2.

Scanning electron microscopy of fracture surfaces showed that failure in all cases had occurred predominantly between lamellae (of which the coating is made up by impact and solidification of impinging molten droplets) or between the lamellae and substrate. The only significant difference observed between the coatings was that the ceramic fracture surfaces showed evidence of brittle fracture of lamellae whereas the metallic coatings showed evidence of plastic deformation of lamellae.

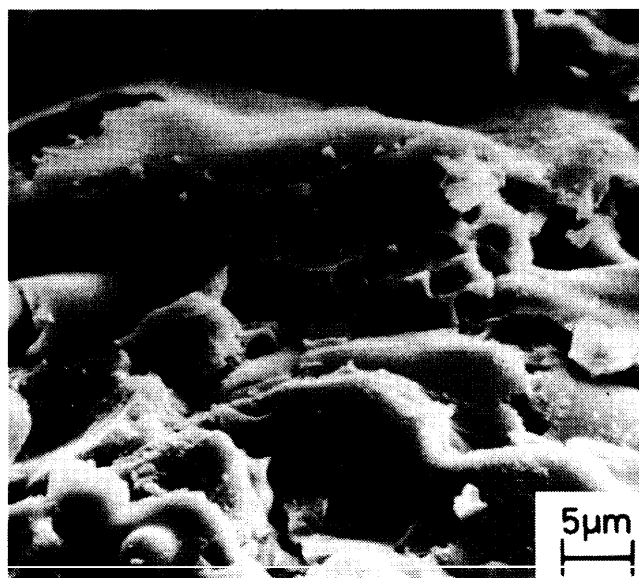


FIG 3 FRACTURE SURFACE OF PLASMA SPRAYED $Al_2O_3-TiO_2$ COATING SHOWING SEPARATION BETWEEN LAMELLAE AND FRACTURE WITHIN LAMELLAE

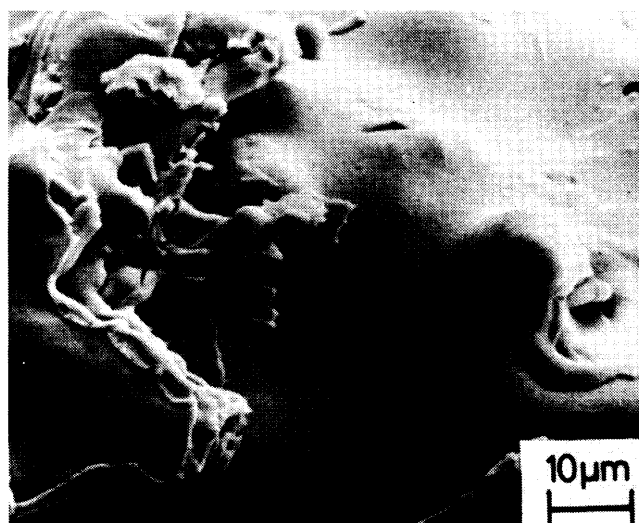


FIG 4 FRACTURE SURFACE OF PLASMA SPRAYED MILD STEEL COATING SHOWING SEPARATION BETWEEN LAMELLAE AND DEFORMATION OF LAMELLAE

4 DISCUSSION

The values of G observed for the various coatings are consistent with their observed service behaviour, that is, both the cohesive and adhesive values for the ceramic are lower than the values for the metallic coatings. The adhesive G for the ceramic and the steel coatings were lower than for cohesive failure, that is failure tends to occur at the coating-substrate interface rather than within the coating. The adhesive G for Ni-Al on steel is very high. The G values for failure at the interface between $\text{Al}_2\text{O}_3\text{-TiO}_2$ and a Ni-Al subcoat are higher than for adhesive or cohesive failure of the ceramic coating on steel. The G values obtained therefore appear to be measuring the "adhesion" of the various coatings.

The higher G values for metallic coatings than for ceramics can be explained by dissipation of energy during plastic deformation of the lamellae in the former, an effect which cannot occur in the latter. The adhesion of ceramic coatings is therefore intrinsically lower than metallic coatings.

The role of a metallic subcoating in improving the adhesion of ceramics can also be explained along similar lines. Failure in the vicinity of the bond-coat interface results in dissipation of energy by deformation of the metallic lamellae as the crack passes between lamellae in both layers, an effect which cannot occur at the interface between a ceramic and solid metallic substrate. Thus G for failure between the subcoat and ceramic is considerably higher than G for ceramic sprayed directly onto steel and the overall adhesive behaviour of the composite coating is enhanced.

The Ni-Al coating provides interesting results because G_a (adhesive) on steel is so much higher than G_c (cohesive). The excellent bonding characteristics of sprayed composite Ni-Al are well known and this has been explained by formation of a metallurgical bond between the substrate and coating [5], although a definite reaction layer has not been observed in other work [7]. The very high G_a compared with G_c however suggests that such a metallurgical bond does not occur to the same extent between lamellae. In view of heat transfer considerations between impacting particles and substrate [8] it is difficult to see how an observable reaction layer could be formed between the substrate and spreading particle in the time available unless the exothermic reaction between Ni and Al continued at a high temperature whilst the droplet was actually spreading. This would suggest however that a similar bond should be formed between lamellae. An alternative explanation for the effectiveness of the bond between Ni-Al and steel could be the alumino-thermic reduction of the thin forming intimate metallic content [8]. This could not happen between lamellae within the coating because frozen particles would be covered by a thick Al_2O_3 film.

Theories of adhesion suggest that, if wetting takes place between liquid and substrate, the molecular interactions after solidification are sufficient to explain the observed adhesive strength. Thus poor adhesion is associated with limited interfacial contact [9]. There seems little doubt that good wetting is a necessary condition but there is some controversy as to whether it is a sufficient condition [10].

The simplest type of coating behaviour to consider is the cohesive failure of alumina for which there is no problem with oxide films between lamellae, as there is for metals; the liquid should wet the previously solidified solid, and the solid is very brittle so that plastic deformation effects can be ignored. The measured value of $G \approx 20 \text{ Jm}^{-2}$ for cohesive failure of the alumina coating may be compared with results from fracture experiments [11] of sintered alumina of $\approx 40 \text{ Jm}^{-2}$. These are of course not

directly comparable because sintered alumina consists of $\alpha\text{-Al}_2\text{O}_3$ whereas the coating is $\gamma\text{-Al}_2\text{O}_3$, and the coating has a lamellar structure which might tend to give higher G values than sintered Al_2O_3 because of crack branching. Nevertheless, this comparison suggests that good contact is made over a large proportion of the apparent area between lamellae and the fracture properties are controlled by defects at the interface. Indeed some recent studies by transmission electron microscopy of ion beam thinned transverse sections of Al_2O_3 coatings have shown regions of good contact and regions in which small gaps ($<0.1 \mu\text{m}$ wide) exist between adjacent lamellae [12]. These defects between lamellae probably arise from ineffective flow of gas from the interface between rapidly spreading molten droplets and previously solidified material [8]. The lower values of G_a for Al_2O_3 on steel are consistent with less effective wetting.

In the case of mild steel and Ni-Al coatings the very low G_c compared with that expected for the bulk material is consistent with poor contact between lamellae because of oxide and entrapped gas. On the other hand the very high G_a for Ni-Al on steel suggests that good contact has been achieved between steel and the impinging droplets, an effect which may be due to chemical interaction between the molten droplet and oxide film on the steel surface.

4 CONCLUSIONS

The fracture mechanics parameters (G_a and G_c) for plasma sprayed coatings provide a guide to their fracture behaviour in practical situations and may be interpreted in terms of energy dissipation processes during crack propagation. Thus plastic deformation of lamellae during fracture of metallic coatings provides a process for energy dissipation which results in a higher resistance to cohesive and adhesive failure than for ceramic coatings. Similarly the previously unexplained ability of metallic subcoats to improve the adhesion of ceramic coatings may be rationalised in terms of energy dissipation by plastic deformation as a crack propagates in the vicinity of the interface between ceramic and subcoat.

The interfaces between lamellae or between lamellae and substrate must be regarded as the "weak links" in determining G_c and G_a so that attempts to improve the mechanical behaviour of coatings should be aimed at improving effective interfacial contact. This is limited in plasma spraying because of adsorbed or entrapped gases and oxide films.

REFERENCES

- 1 Gerdeman, D.A., and Hecht, N.L., "Arc Plasma Technology in Materials Science" (Springer-Verlag, New York, 1972).
- 2 Berndt, C.C., and McPherson, R., 9th Int. Thermal Spraying Conf., The Hague (1980) preprint Vol. p. 310.
- 3 Berndt, C.C., and McPherson, R., "Materials Science Research", Vol. 14 (Eds.) J. Pask and A. Evans, Plenum Press, New York, 1981. p. 619-628.
- 4 Berndt, C.C., and McPherson, R., *Trans. Instn. Engrs. Aust.* ME6 (1981), 53-58.
- 5 Lawn, B.R., and Wilshaw, T.R., "Fracture of Brittle Solids" (Cambridge University Press, Cambridge, 1975).
- 6 Longo, F.N., *Weld. Res. Supplement*, 45, 66S (1966).
- 7 Knotek, O., Lugscheider, E., Cremen, K.H., and Lehrstuhl, B., 9th Intl. Thermal Spraying Conf., The Hague, 1980, preprint Vol. p. 281.
- 8 McPherson, R., *Thin Solid Films*, 83, (1981), 297-310.
- 9 Huntsberger, J.R., "Treatise on Adhesion and Adhesives", Vol. I, (Ed) R.L. Patrick (Edward Arnold, London, 1967) p. 119.
- 10 Bickerman, J.J., "The Science of Adhesive Joints" (Academic Press, New York 1968). p. 137.
- 11 Davidge, R.W., in "Fracture Mechanics of Ceramics", Vol. 2 edited by R.D. Bradt, D.P.H. Hasselman and F.F. Lange (Plenum Press, New York, 1974), p. 447.
- 12 McPherson, R., and Shafer, B.V., *Thin Solid Films* in press.

CAROL
BERNDT

AUSTRALIAN WELDING RESEARCH

CONTENTS

- 1 Photoelastic Determination of Stress Intensity Factors – AWRA Contract 53
By N.L. Svensson
- 10 Variations in the Chemical Composition and Generation Rates of Fume from Different AC Arc Welding Conditions – AWRA Contract 90
By R.K. Tandon, P.T. Crisp, J. Ellis and R.S. Baker
- 15 Testing of Standardised Connections – AWRA Contract 76
By L. Pham and D.S. Mansell
- 23 Adhesion of Thermally Sprayed Coatings – AWRA Contract 81
By C.C. Berndt and R. McPherson
- 26 Implant Testing of Steels – AWRA Contract 74
By J.B. Wade
- 32 Basic Concept of Codes for Welded Construction
By J.B. Wade and A. Vettors
- 35 Strength Characteristics of Adhesive Joints in PVC – AWRA Contract 69
By Yue Chee Yoon
- 42 Effect of Deliberately Induced Damage on the Burst Performance of LPG Cylinder
By A.J. McLead
- 48 Stress Corrosion Cracking in the Weld Metal, Heat Affected Zone and Base Metal of a Line Pipe Weld – AWRA Contract 65
By B.G. Ackland and B.W. Cherry
- 55 Effect of Diameter and Thickness on Hot Tapping Practise – AWRA Contract 84
By J.B. Wade
- 57 The Effect of Fillet Weld Termination on Cyclic Strength of Longitudinal Fillet Welded Joints in Aluminium – AWRA Contract 68
By J.A. Lewis
- 63 Fracture Toughness Properties of Some Australian Electroslag Welds – AWRA Contract 91
By J. Barclay
- 69 Weld Variability – AWRA Contract 96
By D.S. Mansell
- 72 The Welding of Reinforcing Steel – AWRA Contract 64
By D.J.H. Corderoy and H. Pearson

